

C₆₀-induced reconstruction of the Ge(111) surface

Hang Xu

*Rowland Institute for Science, Cambridge, Massachusetts 02142-1297
and Physics Department, Harvard University, Cambridge, Massachusetts 02138*

D. M. Chen* and W. N. Creager

Rowland Institute for Science, Cambridge, Massachusetts 02142-1297

(Received 7 April 1994)

We report a direct observation of surface reconstruction induced by the adsorption of C₆₀ molecules. At submonolayer and full monolayer coverage of C₆₀ on Ge(111), two surface phases ($3\sqrt{3}\times 3\sqrt{3}R30^\circ$ and $\sqrt{13}\times\sqrt{13}R14^\circ$) as well as a localized metastable 5×5 phase are identified by low-energy electron diffraction and scanning tunneling microscopy. The formation of the two phases is facilitated by induced reconstructions of the Ge surface into different surface structures. Models for these surface structures are proposed that elucidate the close interplay between the adsorbed C₆₀ molecules and the host Ge surface.

I. INTRODUCTION

The recent discovery of superconductivity and other fascinating properties of C₆₀-based materials^{1,2} has stimulated a large number of experimental investigations on the adsorption of C₆₀ molecules and the growth of C₆₀ thin films on surfaces of metals,³⁻⁵ semiconductors,⁶⁻⁹ and insulators.¹⁰⁻¹² An important goal of the research in this area is to understand the interfacial interactions. A C₆₀ molecule, consisting of 60 long single bonds and 30 short double bonds, has two sets of low-lying triply degenerate unoccupied molecular orbitals and a large electron affinity.^{2,13} Such a unique electronic structure leads to several possible interaction mechanisms between a C₆₀ and a surface. C₆₀ molecules are believed to be bonded on an inert surface such as GeS (Ref. 12) by van der Waals forces just like the intermolecular forces in a C₆₀ solid.¹⁴ Charge transfer from metal surfaces to C₆₀ adsorbates, resembling that in the alkali-metal-doped C₆₀ solid,¹ have been reported.¹⁵ On semiconductor surfaces, charge transfer¹⁵ and local chemical-bond formation are both probable. A comprehensive understanding of this problem is still a matter under pursuit.

From the structural point of view, the rigid truncated icosahedral geometry of the C₆₀ plays important roles in the adsorption processes as well. The geometrical constraint imposed between the pseudospherical molecule surface and the two-dimensional (2D) solid surface allows only a few carbon atoms on each molecule to be in contact with the substrate. To enhance the binding, the C₆₀ molecules could choose an optimal orientation, and, in extreme cases, structural instability of the surface could be introduced. For example, Cu(111) has been reported to induce orientational ordering of a commensurate 5×5 C₆₀ overlayer,³ yet on Au(111) and Au(110) changes of the underlying Au structures have been observed upon the adsorption of C₆₀ molecules.^{4,5}

In this paper we report a direct observation of C₆₀-

induced surface reconstruction of a Ge(111) surface. Using low-energy electron diffraction (LEED) and scanning tunneling microscopy (STM) techniques, we show that various C₆₀ deposition and annealing procedures produce two surface phases ($\sqrt{13}\times\sqrt{13}R14^\circ$ and $3\sqrt{3}\times 3\sqrt{3}R30^\circ$) and one localized metastable structure (5×5) on a Ge(111) surface. The formation of these three phases requires reconstructions of the virgin $c(2\times 8)$ surface into various configurations that accommodate the C₆₀ ad molecules as an ordered discrete array, a 2D layer, and a 2D network, respectively. These C₆₀-induced surface reconstructions are in sharp contrast to the behavior of C₆₀ molecules adsorbed on Si surfaces,^{8,9} where only disordered layers of C₆₀ were observed at submonolayer coverage, leaving the silicon substrate unaltered. In fact, similar C₆₀-induced structural instabilities have not been observed on any of the semiconductor surfaces studied in previous experiments. The close interplay between C₆₀ molecules and the Ge substrate that lowers the overall surface energy is quite intriguing and deserves further theoretical analysis.

II. EXPERIMENT

The specimens were prepared and characterized for this experiment in a UHV system with a base pressure below 10^{-10} torr. Typically, a piece of Ga-doped Ge(111) wafer (0.2 Ω cm) was outgassed overnight by resistive heating, then sputtered at room temperature and annealed at $\sim 700^\circ\text{C}$ for two to three cycles, resulting in a clean $c(2\times 8)$ surface as confirmed by Auger spectroscopy, LEED pattern, and STM images. The clean Ge surface was then exposed to a flux of C₆₀ molecules sublimed at a rate of 0.05 ML/min from an effusion cell held at 400°C .¹⁶ The substrate was held between 20°C and 200°C during the deposition and subsequently annealed in a wide range of temperatures. Different C₆₀ deposition densities and annealing procedures produced different

surface phases. Two commercial fullerene sources containing 1% and 10% C₇₀ impurities among the C₆₀ molecules were used with essentially the same results. All tunneling images were acquired at room temperature, with a constant current set between 10–50 pA and a tip bias of –2.0 to –3.0 V.

III. ORDERED SURFACE STRUCTURES

The LEED patterns and STM images associated with clean Ge(111) $c(2\times 8)$ surfaces are well documented.¹⁷ The inset of Fig. 1(a) shows a typical triple-domain $c(2\times 8)$ LEED pattern. Upon the adsorption of C₆₀ on the clean surface held at room temperature, the $c(2\times 8)$ LEED pattern becomes gradually diffuse and only weak 1×1 diffraction spots are visible at 1-ML coverage. STM images reveal that C₆₀ molecules distribute randomly on the Ge substrate. Occasional local ordering of a few

closely packed molecules was also observed. This behavior is similar to the adsorption of C₆₀ on silicon surfaces.^{8,9}

Substantial ordering was observed after prolonged 250°C annealing of a sample covered with 1 ML of C₆₀, as indicated by an emerging LEED pattern. The pattern evolves continuously at higher annealing temperatures up to roughly 500°C. The final LEED pattern, shown in Fig. 1(a), indicates that the original $c(2\times 8)$ surface structure has now been replaced by a $3\sqrt{3}\times 3\sqrt{3}R30^\circ$ (henceforth $3\sqrt{3}$) structure. A typical real-space STM image is shown in Fig. 1(b). This $500\times 500\text{-\AA}^2$ image shows a number of Ge terraces predominantly covered by C₆₀ molecules with a few brighter C₇₀ impurities interspersed. The structure consists of numerous small translational domains. Within each domain, the C₆₀ molecules are separated by $\sim 10\text{ \AA}$ and packed in closed hexagons with the short diagonal axes running parallel to the bulk $[11\bar{2}]$ direction, an arrangement similar to that of the (111) surface of an fcc C₆₀ crystal.^{7–9} These charac-

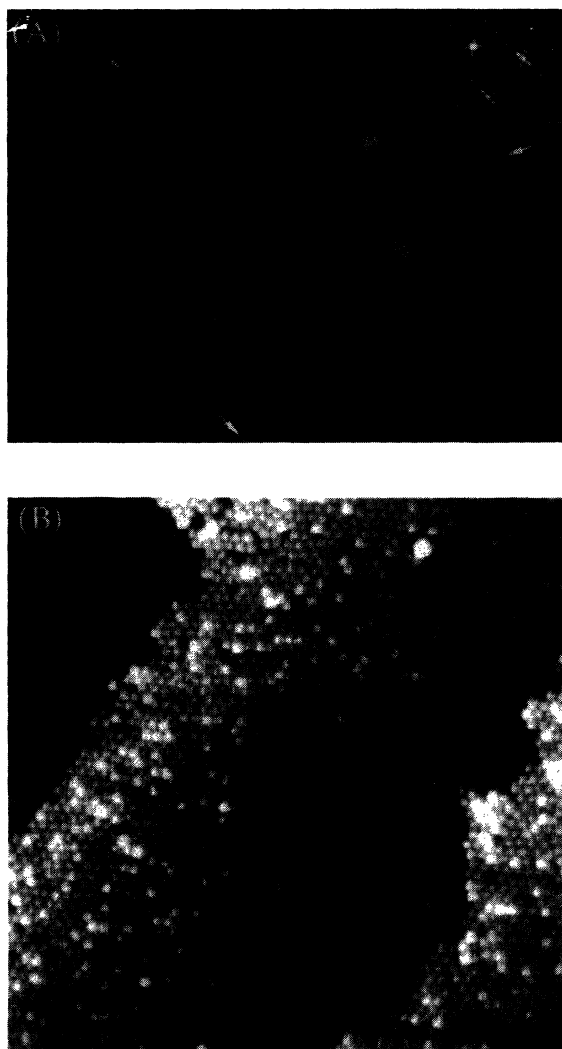


FIG. 1. (a) The LEED pattern at 32-eV incident electron energy. The arrows point to the first-order spots. The inset shows the LEED pattern of the Ge(111) $c(2\times 8)$ surface taken at the same electron-beam energy. (b) A $500\times 500\text{-\AA}^2$ STM image of the $3\sqrt{3}\times 3\sqrt{3}R30^\circ$ phase.

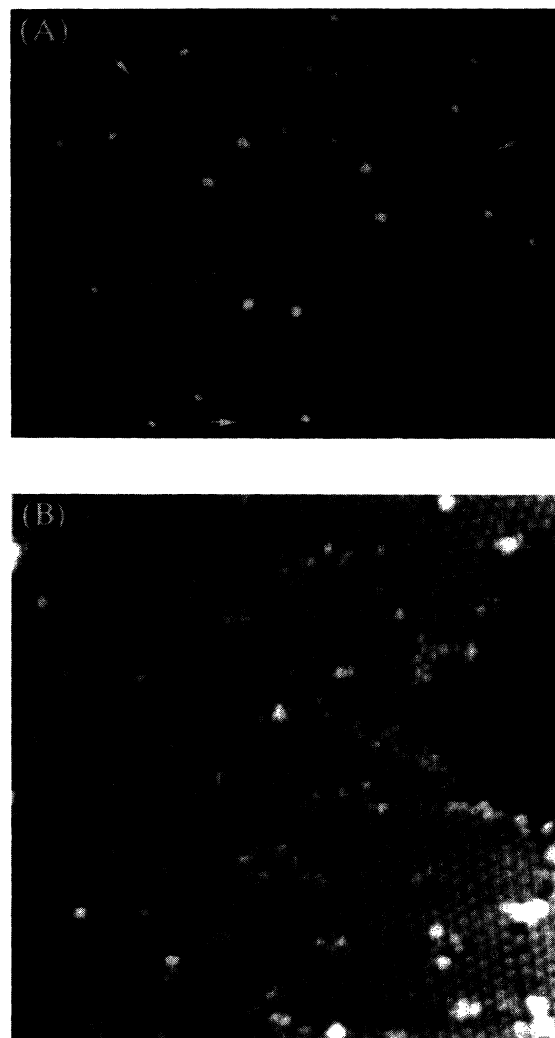


FIG. 2. (a) The LEED pattern at 41-eV incident electron energy. The arrows indicate the first-order spots. (b) A $500\times 500\text{-\AA}^2$ STM image of the $\sqrt{13}\times \sqrt{13}R14^\circ$ phase.

teristics account well for the relatively poor diffraction quality and for the 30° rotation of the surface structure relative to the bulk lattice as exhibited in the LEED pattern. However, the periodicity of the observed C_{60} overlayer structure in the STM images is twice the periodicity of the LEED pattern. As will be shown in the next section, this "discrepancy" is a clear indication that the underlying Ge substrate has undergone a reconstruction.

The degree of ordering of the $3\sqrt{3}$ structure cannot be improved further by increasing the annealing temperature. Instead, when the temperature exceeds a critical value around 500°C , an abrupt change in the LEED pattern occurs. Within seconds, the $3\sqrt{3}$ pattern is completely transformed into another and much sharper pattern, as shown in Fig. 2(a). This process is accompanied by a decrease in the carbon peak with respect to the Ge peak in the Auger spectra, signifying partial desorption of the C_{60} molecules from the $3\sqrt{3}$ surface. This LEED pattern can be decomposed into two subsets, each with a $\sqrt{13}\times\sqrt{13}$ structure but rotated either $+13.9^\circ$ or -13.9° from the bulk $[11\bar{2}]$ axis. Indeed, the STM images reveal that the entire surface is divided into many arbitrarily mixed translational domains with two distinct orientations. Figure 2(b) is a typical STM image of $500\times 500 \text{ \AA}^2$, where individual molecules are clearly resolved. The upper-left part contains five translational domains with the same orientation while the lower part displays several domains with a different orientation. Apart from the 27.8° relative rotation, the C_{60} lattices of all the domains are identical. It is a hexagonal-close-packed array with an intermolecular distance of 14.4 \AA . We label this phase $\sqrt{13}\times\sqrt{13}R 14^\circ$ (or $\sqrt{13}$ in short).

The $\sqrt{13}$ phase remains stable up to 700°C , the full C_{60} desorption temperature, above which the Ge surface reconstructs back to its original $c(2\times 8)$ structure. It is possible, however, to obtain a surface with coexisting phases by flash annealing to 700°C and quenching a sample originally covered with 1 ML of C_{60} . The STM image shown in Fig. 3(a) is one example exhibiting the $3\sqrt{3}$ phase, the $\sqrt{13}$ phase, and the restored $c(2\times 8)$ phase. The absence of impurity clusters or islands in many of these pictures suggests that dissociation of C_{60} molecules during heating is very unlikely. Although the large number of translational domains in the $3\sqrt{3}$ phase might be attributed to a kinetic effect below the partial desorption temperature, the similar behavior in the $\sqrt{13}$ phase is more likely an indication of relatively small domain-wall energy. From a topological point of view, as many as 26 types of domain boundaries could be present in the $\sqrt{13}$ phase. Prolonged annealing does produce larger domains, but the overall surface morphology remains nearly the same.

Quenching the $3\sqrt{3}$ sample heated briefly to about 500°C yields yet another localized 5×5 structure revealed only by STM. In this structure, the C_{60} molecules form a 2D network as shown in Fig. 4(b). It may also be viewed as a hexagonal array of vacancies in a closely packed C_{60} layer. Measurement of the corrugations in the STM images shows that the rows of the molecules display a slight zigzag pattern, and their average posi-

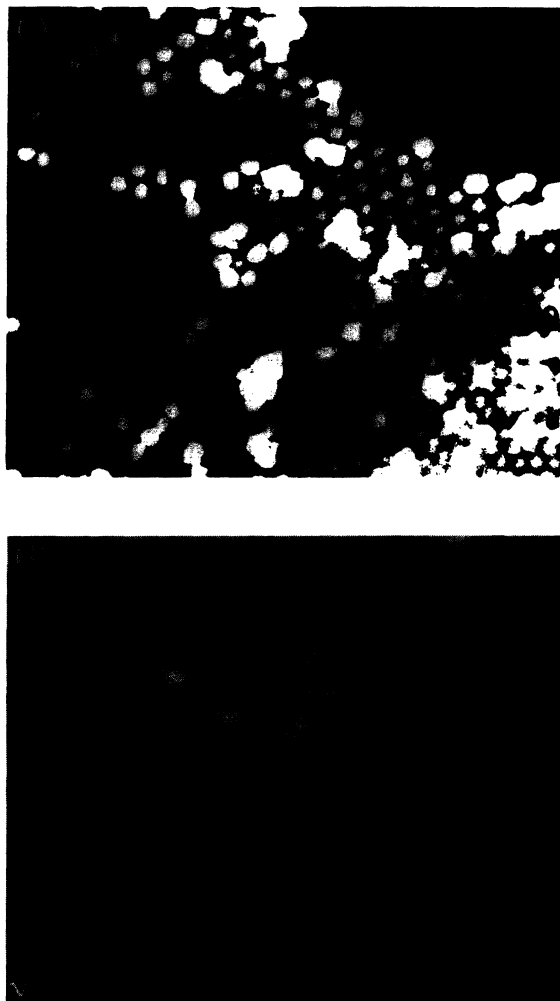


FIG. 3. (a) A $350\times 300\text{-\AA}^2$ STM image of the flash-annealed surface showing both the $3\sqrt{3}\times 3\sqrt{3}R 30^\circ$, and the $\sqrt{13}\times\sqrt{13}R 14^\circ$ phases, as well as part of a restored Ge(111) $c(2\times 8)$; (b) a $350\times 300\text{-\AA}^2$ STM image of the 5×5 network structure together with the $\sqrt{13}\times\sqrt{13}R 14^\circ$ phase.

tions are aligned with the bulk $[\bar{1}10]$ axes. Unlike the previous two phases, no LEED pattern associated with this 5×5 structure was observed, due to the small fraction of the 5×5 domains. It is possible that this metastable structure exists in a very narrow range of coverage and temperature.

To summarize, under different sample preparation procedures, C_{60} molecules can form three ordered surface structures on the Ge(111) surface: $3\sqrt{3}\times 3\sqrt{3}R 30^\circ$, $\sqrt{13}\times\sqrt{13}R 14^\circ$, and localized 5×5 .

IV. SUBSTRATE RECONSTRUCTION

The above three surface structures exhibit distinct characteristics. While the molecules in the $\sqrt{13}$ phase register in a discrete array with a large intermolecular spacing, they form a 2D network in the 5×5 structure, and a hexagonal-close-packed overlayer in the $3\sqrt{3}$ phase. Although all three structures consist of translational

domains or rotational domains, the sizes of these domains have no correlation with the original triple domains of the $c(2 \times 8)$ Ge surface. To accommodate these diverse C_{60} structures, it would be necessary for the host Ge surface to undergo reconstructions. Indeed, the fast deterioration and eventual disappearance of the $c(2 \times 8)$ LEED pattern of a clean Ge surface upon the adsorption of C_{60} molecules near room temperature already suggest that some local rearrangement of the host Ge atoms is taking place as the deposition of C_{60} molecules proceeds.

A more direct indication of the C_{60} -induced reconstruction of the Ge surface comes from the fact that for the $3\sqrt{3}$ structure, top-layer C_{60} molecules in the STM image [Fig. 1(a)] display twice the periodicity as the one given by the LEED pattern. This observation is further supported by the Fourier transformation of several STM images like the one in Fig. 1(a), which yields only $3\sqrt{3}/2 \times 3\sqrt{3}/2$ spots. Thus the observed $3\sqrt{3} \times 3\sqrt{3}$ periodicity in the LEED pattern can only be derived either from the underlying Ge lattice alone, or from both the Ge substrate and the C_{60} overlayer with multiple scattering taken into account. It is easy to show that no combination of a $3\sqrt{3}/2 \times 3\sqrt{3}/2 R 30^\circ$ C_{60} structure and the $c(2 \times 8)$ Ge structure can reproduce a $3\sqrt{3} \times 3\sqrt{3} R 30^\circ$ LEED structure.¹⁸ Therefore, for the $3\sqrt{3}$ phase, the underlying Ge structure must be one other than the virgin $c(2 \times 8)$ structure.

In principle, however, the discrepancy between the periodicity of the STM image and that of the LEED pattern could be reconciled if alternating molecules exhibit two distinct orientations that could only be detected by LEED, not STM. Although orientation ordering due to intermolecular interactions in a C_{60} solid does not occur at room temperature,¹⁹ such ordering for C_{60} molecules on surfaces could be induced by substrate atoms. Since the $c(2 \times 8)$ structure possesses neither the right periodicity nor the threefold symmetry of $3\sqrt{3} \times 3\sqrt{3} R 30^\circ$, it is inconceivable for this surface to bind C_{60} molecules with an orientational order and the overall $3\sqrt{3} \times 3\sqrt{3} R 30^\circ$ structure. Under these considerations, a different Ge substrate structure should also be in order.

The $3\sqrt{3} \times 3\sqrt{3}$ reconstruction takes place *continuous-*

ly from 250°C to near 500°C. At 500°C the transition from the $3\sqrt{3}$ phase to the $\sqrt{13}$ phase occurs *abruptly*. On the other hand, we were not able to trigger a reverse transition from $\sqrt{13}$ to $3\sqrt{3}$ phase by manipulating the C_{60} coverage or the annealing temperature. Alternatively, the $\sqrt{13}$ phase can be produced by directly depositing C_{60} onto the clean $c(2 \times 8)$ surface held near the transition temperature. It is well known that above 300°C (Refs. 20 and 21) the $c(2 \times 8)$ structure of Ge(111) becomes disordered. This means that the $\sqrt{13}$ structure can form on an initially disordered Ge surface at elevated temperature, and the Ge atoms are frozen into an ordered structure due to the termination of C_{60} molecules. Once formed, the $\sqrt{13}$ phase remains stable until desorption occurs at 700°C, almost 400°C higher than the melting temperature of a naked Ge surface. Because of the weak C_{60} - C_{60} coupling associated with large intermolecular spacing in the $\sqrt{13}$ structure, the much enhanced stability of this phase must come primarily from a unique local C_{60} -Ge arrangement. From these observations, together with the LEED and STM results, we conclude that the underlying Ge lattice of the $\sqrt{13}$ phase has a $\sqrt{13} \times \sqrt{13} R 14^\circ$ structure. Likewise, we believe that the Ge substrate in the localized 5×5 domain has a 5×5 structure.

V. MODELING AND DISCUSSIONS

It is quite remarkable that on a Ge surface alone, C_{60} molecules can be arranged in a discrete array ($\sqrt{13}$), a close-packed layer ($3\sqrt{3}$), as well as a 2D network (5×5) through the C_{60} -induced reconstruction of the host surface. To appreciate how the Ge surface accommodates these different configurations, we have constructed models for all three structures. These models are shown along with several native Ge surface structures in Fig. 4, where the Ge adatoms are represented by small gray circles atop the small open and solid circles of the bilayer, and the larger bold circles are the C_{60} ad molecules. Table I summarizes the unit-cell dimensions and the density of adatoms, rest atoms, and ad molecules for the various models.

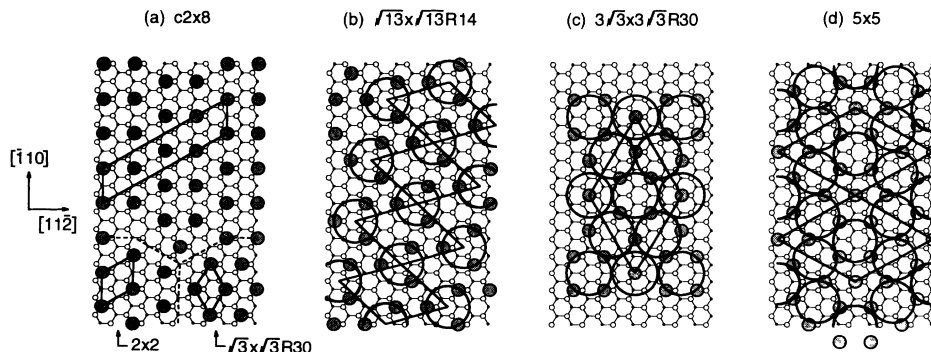


FIG. 4. The widely accepted model for (a) the Ge(111) $c(2 \times 8)$, and proposed models for (b) the $\sqrt{13} \times \sqrt{13} R 14$, (c) the $3\sqrt{3} \times 3\sqrt{3} R 30$, and (d) the 5×5 structures. The C_{60} molecules are represented by 10-Å large open circles scaled in proportion to the Ge(111) bilayer shown in small open and solid circles in descending order. The Ge adatoms are represented by shaded circles, which are sandwiched in between the C_{60} and the Ge bilayer.

TABLE I. Proposed unit-cell size, number of Ge adatoms, Ge rest atoms, and C_{60} 's per Ge 1×1 cell for the three models in Fig. 4, compared with those of the widely accepted $c(2 \times 8)$ model.

	Unit cell (Å)	Ge adatoms	Ge rest atoms	C_{60} molecules
$c(2 \times 8)$		$\frac{1}{4}$	$\frac{1}{4}$	
$\sqrt{13} \times \sqrt{13} R 14$	14.4	$\frac{3}{13}$	$\frac{4}{13}$	$\frac{1}{13}$
$3\sqrt{3} \times 3\sqrt{3} R 30$	10.24	$\frac{7}{27}$	$\frac{6}{27}$	$\frac{4}{27}$
5×5	9.85	$\frac{7}{25}$	$\frac{4}{25}$	$\frac{3}{25}$

In addition to the constraints imposed by the above LEED and STM results, we also took into account two other factors in our modeling. First, the STM images show that C_{60} -induced reconstructions do not lead to nucleation of other terraces, nor to severe roughening of the step edges. This implies that the Ge adatom density is roughly conserved. Second, to minimize the strain, Ge adatoms should maintain a triple back-bond structure similar to that found in the $c(2 \times 8)$ structure [Fig. 4(a)], while the C_{60} molecules should favor threefold or fourfold adsorption sites.⁸ The information summarized in Table I shows that the models proposed in Figs. 4(b)–4(d) meet these criteria reasonably well. It is evident in Fig. 4 that the reconstructed Ge surfaces incorporate naturally elements of the $c(2 \times 8)$, 2×2 , and $3\sqrt{3} \times 3\sqrt{3} R 30^\circ$ structures shown in Fig. 4(a).

For the $\sqrt{13}$ phase, the second rotational domain can be readily generated via simple mirror operation. In this model, each C_{60} molecule is supported by three Ge adatoms and is essentially isolated from its neighboring molecules because of the 14.4-Å separation from one another. The C_{60} -3Ge clusters are the essential building blocks of this structure. In contrast, in the $3\sqrt{3}$ phase, the C_{60} molecules are in close contact and the interaction between the molecules should also play a role in stabilizing the final structures. Thus, the model in Fig. 4(c) for the $3\sqrt{3}$ phase suggests that each of the C_{60} molecules atop a Ge adatom is pinned in place by three C_{60} molecules resting on fourfold sites. For the underlying Ge lattice, we favor a $3\sqrt{3} \times 3\sqrt{3} R 30^\circ$ structure over a $\sqrt{3} \times \sqrt{3} R 30^\circ$ structure for the following two reasons. First, C_{60} molecules do not form ordered structures on a boron-induced Si(111)- $\sqrt{3} \times \sqrt{3}$ surface;²² second, the $3\sqrt{3} \times 3\sqrt{3}$ structure in the model can retain the local structure of the original $c(2 \times 8)$ surface quite well. It is interesting to note that the Ge adatom configuration in the 5×5 model is a reduced copy of that in the $3\sqrt{3}$ model. If the C_{60} nearest-neighbor distance could be reduced by 4% (10.0 versus 10.4 Å), we would then have a similar C_{60} layer arrangement for the 5×5 structure as for the $3\sqrt{3}$ phase, except for a 30° rotation. Such compression is not energetically favored, though. Consequently, the six molecules surrounding each corner of the 5×5 unit cell contract inward or expand outward alternately at the expense of removing the corner molecules, resulting in the observed network structure. The above manifestation of

the close interplay between the C_{60} molecules and the Ge surface is quite intriguing, and it is not unlikely that there exist other possible structures yet to be observed.

In the preceding models, we have not specified the C_{60} orientations relative to the surface. To do so would require knowledge about the C_{60} -Ge binding mechanism for these phases, which entails further theoretical analysis. Because of the high electron affinity of the C_{60} molecule,² it is tempting to speculate that electronic charge is transferred from the Ge atoms to the triply degenerate lowest empty orbitals of the C_{60} molecules. The resultant ionic bonding might be a possible explanation for the remarkable structural flexibility demonstrated by this system. However, tunneling spectra measured over C_{60} molecules on all three structures show a well-defined gap of ~ 2 eV, and thus, at best, could only support a localized charge-transfer mechanism. In fact, if significant delocalized charge transfer would take place, the C_{60} molecules should experience a lateral repulsion from the neighboring molecules and the molecules along the domain boundaries may be forced out of registry, especially for the $3\sqrt{3}$ and 5×5 structure. This is clearly not the case as shown by all the tunneling images.

Another possible binding mechanism is to form local C-Ge-C or Ge-C bonds at the interface by severing C-C double bonds on the C_{60} molecule. Although this type of reaction is responsible for the formation of many of the C_{60} derivatives,²³ it is subject to the geometrical constraint imposed between the 2D atomic surface and the pseudospherical C_{60} molecule structure. It is nontrivial to obtain a close match of atomic locations, bond lengths, and bond angles between the substrate and C_{60} ad-molecules. Presently, we do not have satisfactory alternative models at this level to replace those shown in Fig. 4.

VI. CONCLUSIONS

We have observed two surface phases, $3\sqrt{3} \times 3\sqrt{3} R 30^\circ$ and $\sqrt{13} \times \sqrt{13} R 14^\circ$, and a localized metastable 5×5 structure on a C_{60} -terminated Ge(111) surface. We have shown that the C_{60} -induced surface reconstruction is essential to enable the Ge(111) surface to accommodate three very different C_{60} -Ge configurations. We have constructed models that agree well with the experimental results. Further investigations, especially experimental determination of the surface electronic structures and the underlying Ge surface structures are needed to verify these models and to reach a sound understanding of the interfacial-binding mechanism.

ACKNOWLEDGMENTS

We thank J. Golovchenko for suggesting multiple-scattering analysis of the LEED pattern, M. Nilsson and J. Scarpetti for their photographic work, and A. Stern for technical assistance in the Fourier transform of STM images. The support provided to H.X. by the Rowland Foundation is gratefully acknowledged.

*Author to whom correspondence should be addressed.

- ¹A. F. Hebard, M. J. Rosseinsky, R. C. Haddon, D. W. Murphy, S. H. Glarum, T. T. M. Palstra, A. P. Ramirez, and A. R. Kortan, *Nature* **350**, 600 (1991).
- ²R. C. Haddon, *Acc. Chem. Res.* **25**, 127 (1992).
- ³Tomihiko Hashizume, K. Motai, X. D. Wang, H. Shinohara, Y. Saito, Y. Maruyama, K. Ohno, Y. Kawazoe, Y. Nishina, H. W. Pickering, Y. Kuk, and T. Sakurai, *Phys. Rev. Lett.* **71**, 2959 (1993).
- ⁴J. K. Gimzewski, S. Modesti, T. David, and R. R. Schlittler, *J. Vac. Sci. Technol. B* **12**, 1942 (1994).
- ⁵E. I. Altman and R. J. Colton, *Surf. Sci.* **279**, 49 (1992).
- ⁶Y. Z. Li, J. C. Patrin, M. Chander, J. H. Weaver, L. P. E. Chibante, and R. E. Smalley, *Science* **252**, 547 (1991).
- ⁷Y. Z. Li, M. Chander, J. C. Patrin, J. H. Weaver, L. P. F. Chibante, and R. E. Smalley, *Science* **253**, 429 (1991).
- ⁸Tomihiko Hashizume, Xiang-Dong Wang, Yuichiro Nishina, Hisanoti Shinohara, Yahachi Saito, Young Kuk, and Toshio Sakurai, *Jpn. J. Appl. Phys.* **31**, L880 (1992).
- ⁹Hang Xu, D. M. Chen, and W. N. Creager, *Phys. Rev. Lett.* **70**, 1850 (1993).
- ¹⁰D. Schmicker, S. Schmidt, J. G. Skofronick, J. P. Toennies, and R. Vollmer, *Phys. Rev. B* **44**, 10995 (1991).
- ¹¹T. Ichihashi, K. Tanigaki, W. Ebbesen, S. Kuroshima, and S. Iijima, *Chem. Phys. Lett.* **190**, 179 (1992).
- ¹²J. M. Themlin, S. Bouzidi, F. Coletti, J. M. Debever, G. Genterblum, L. M. Yu, J. J. Pireaux, and P. A. Thiry, *Phys. Rev. B* **46**, 15 602 (1992).
- ¹³L. S. Wang, J. Conceicao, C. Lin, and R. E. Smalley, *Chem. Phys. Lett.* **182**, 5 (1991).
- ¹⁴S. Saito and A. Oshiyama, *Phys. Rev. Lett.* **66**, 2637 (1991).
- ¹⁵T. R. Ohno, Y. Chen, S. E. Harvey, G. H. Kroll, and J. H. Weaver, *Phys. Rev. B* **44**, 13 747 (1991).
- ¹⁶1 ML corresponds to the density of hexagonal-close-packed C₆₀ molecules with 10-Å intermolecular spacing, or, $1.15 \times 10^{14} \text{ cm}^{-3}$.
- ¹⁷R. S. Becker, B. S. Swartzentruber, J. S. Vickers, and T. Klitsner, *Phys. Rev. B* **39**, 1633 (1989).
- ¹⁸Together with a $3\sqrt{3}/2 \times 3\sqrt{3}/2R30^\circ$ C₆₀ structure, only the following three possible Ge substrate structures can yield the $3\sqrt{3} \times 3\sqrt{3}R30^\circ$ LEED pattern: (a) $3\sqrt{3} \times 3\sqrt{3}R30^\circ$, (b) $\sqrt{3} \times \sqrt{3}R30^\circ$, or (c) 3×3 . For (b) and (c), Ge-C₆₀ multiple scattering must be considered [for example, see L. J. Clarke, *Surface Crystallography—An Introduction to Low Energy Electron Diffraction* (Wiley, New York, 1985), p. 22].
- ¹⁹For example, see a recent review by Paul A. Heinley, *The Fullerenes*, edited by H. W. Kroto *et al.* (Pergamon, Oxford, 1993), p. 163.
- ²⁰R. M. Feenstra, A. J. Slavin, G. A. Held, and M. A. Lutz, *Phys. Rev. Lett.* **66**, 3257 (1991).
- ²¹R. J. Phaneuf and M. B. Webb, *Surf. Sci.* **164**, 167 (1985).
- ²²D. M. Chen, H. Xu, W. N. Creager, and P. Burnett *J. Vac. Sci. Technol. B* **12**, 1910 (1994).
- ²³P. J. Fagan, J. C. Calabrese, and B. Malone, *Acc. Chem. Res.* **25**, 134 (1992).

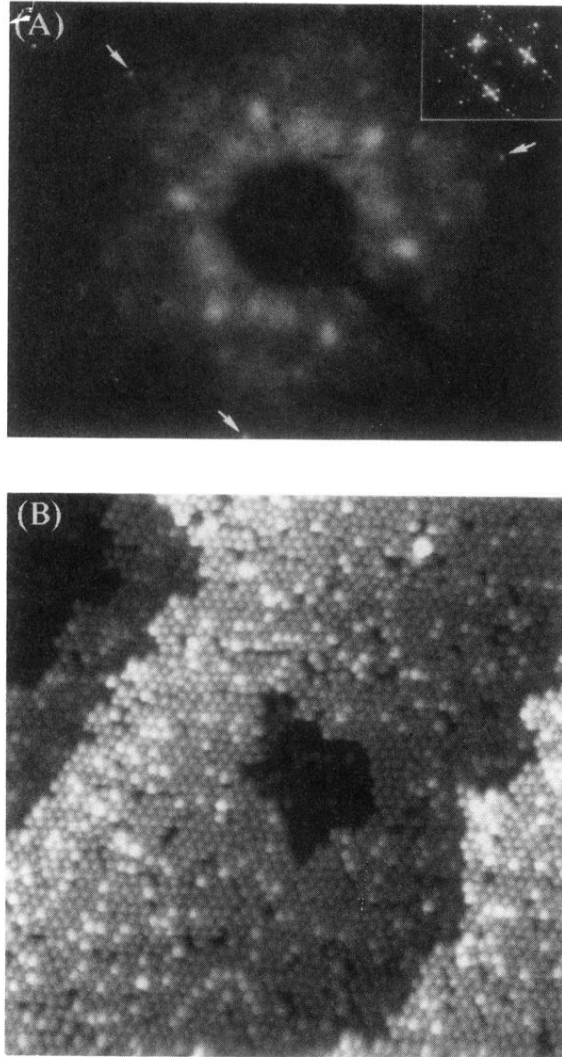


FIG. 1. (a) The LEED pattern at 32-eV incident electron energy. The arrows point to the first-order spots. The inset shows the LEED pattern of the Ge(111) $c(2 \times 8)$ surface taken at the same electron-beam energy. (b) A $500 \times 500\text{-\AA}^2$ STM image of the $3\sqrt{3} \times 3\sqrt{3}R 30^\circ$ phase.

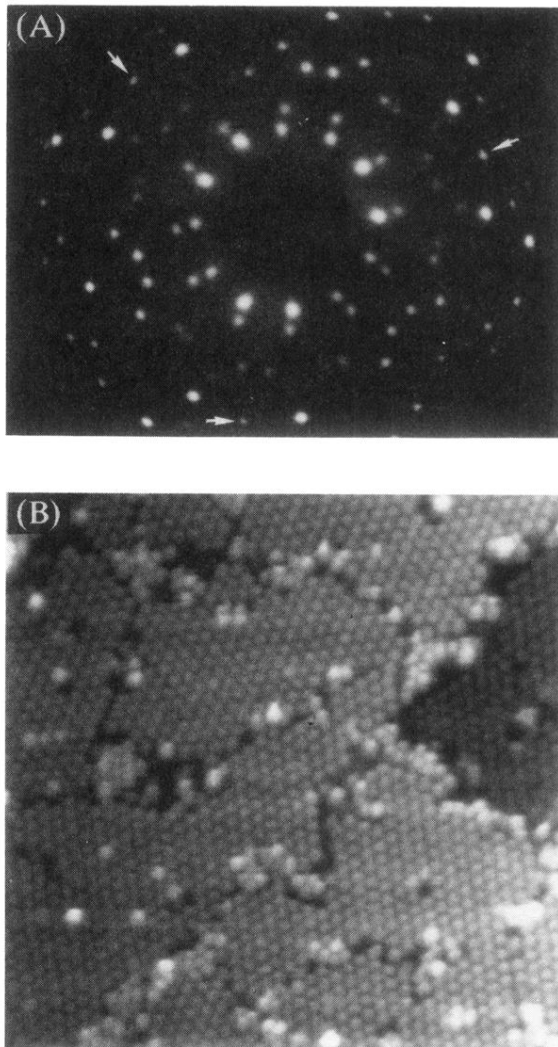


FIG. 2. (a) The LEED pattern at 41-eV incident electron energy. The arrows indicate the first-order spots. (b) A $500 \times 500\text{-\AA}^2$ STM image of the $\sqrt{13} \times \sqrt{13} R14^\circ$ phase.

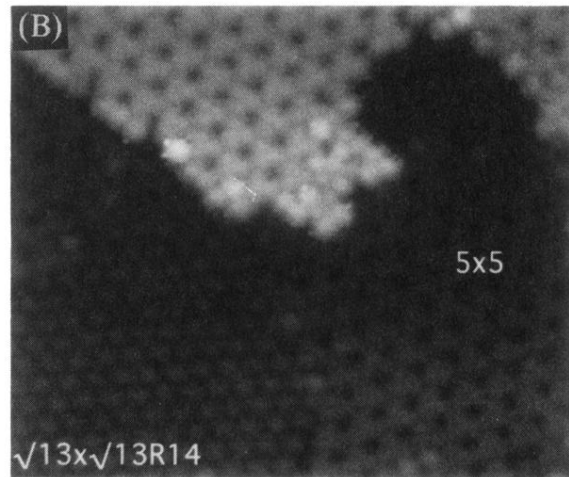
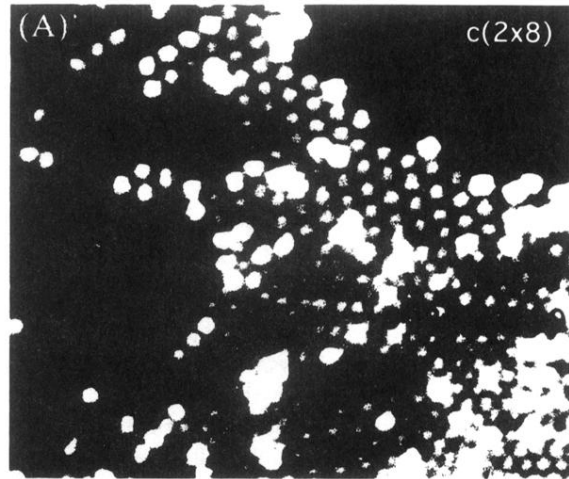


FIG. 3. (a) A $350 \times 300\text{-\AA}^2$ STM image of the flash-annealed surface showing both the $3\sqrt{3} \times 3\sqrt{3} R30$, and the $\sqrt{13} \times \sqrt{13} R14$ phases, as well as part of a restored Ge(111) $c(2 \times 8)$; (b) a $350 \times 300\text{-\AA}^2$ STM image of the 5×5 network structure together with the $\sqrt{13} \times \sqrt{13} R14$ phase.

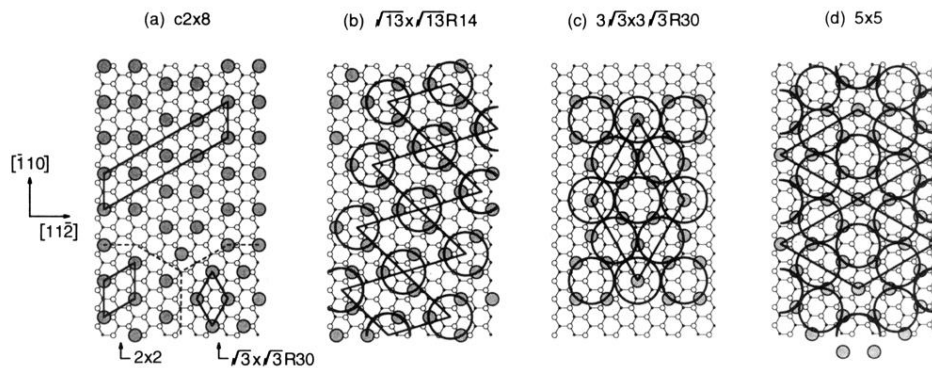


FIG. 4. The widely accepted model for (a) the Ge(111) $c(2 \times 8)$, and proposed models for (b) the $\sqrt{13} \times \sqrt{13} R14$, (c) the $3\sqrt{3} \times 3\sqrt{3} R30$, and (d) the 5×5 structures. The C_{60} molecules are represented by 10-Å large open circles scaled in proportion to the Ge(111) bilayer shown in small open and solid circles in descending order. The Ge adatoms are represented by shaded circles, which are sandwiched in between the C_{60} and the Ge bilayer.